JOURNAL OF THERMOPHYSICS AND HEAT TRANSFER
Vol. 19, No. 4, October–December 2005

Numerical Model for Spray-Wall Impaction and Heat Transfer at Atmospheric Conditions

Roy J. Issa*
West Texas A&M University, Canyon, Texas 79016
and
S. C. Yao†
Carnegie–Mellon University, Pittsburgh, Pennsylvania 15213

A numerical model is developed to simulate for atmospheric applications the impingement of water sprays on surfaces heated at temperatures ranging from nucleate to film boiling. The droplets are modeled in the Lagrangian frame of reference and are dispersed stochastically in the continuous gas phase. The model is based on the fundamental basics of single water droplet impingements extended to full sprays, where the overall heat-transfer process is broken down into its basic components: boiling heat transfer associated with the droplet contact, bulk air convection, and radiation. Droplet dynamics at the wall is modeled based on an empirical correlation relating the droplet incoming to outgoing Weber number. Droplet contact heat transfer is modeled using an effectiveness parameter for the heat transfer that is a function of the droplet Weber number. Numerically modeling the droplet-wall dynamics and contact heat transfer has not been addressed before in a numerical model. The model is tested at atmospheric pressure using experimental data for nozzles that disperse a spectrum of nonuniform droplets. Favorable comparison with the experimental data is demonstrated.

Nomenclature

$c_{p,v}$	=	vapor specific heat constant, J/kg · K
$c_{p,l}$	=	liquid specific heat constant, J/kg · K
d	=	droplet diameter, μm
e_n	=	droplet normal coefficient of restitution
G	=	water mass flow flux, kg/m^2 · s
h_{mist}	=	mist heat-transfer coefficient, W/m^2 · K
h_{total}	=	total heat-transfer coefficient, W/m^2 · K
q_c	=	droplet contact heat flux (also referred to as boiling heat flux), W/m^2
T_{liq}	=	liquid (droplet) temperature, °C
T_{sat}	=	liquid saturation temperature, °C
T_w	=	wall temperature, °C
u_τ	=	shear velocity at the wall, m/s
v	=	droplet velocity at the nozzle exit, m/s
v_a	=	air velocity, m/s
v_i	=	impinging droplet normal velocity component at the surface, m/s
We_n	=	normal component of the impinging droplet Weber number at the surface
y	=	normal distance from the wall, m
Δh_{fg}	=	latent heat of vaporization, J/kg
ε	=	heat-transfer effectiveness
θ_s	=	nozzle-exit spray angle (spray cone angle), deg
μ	=	dynamic viscosity of the liquid-vapor mixture, kg/s · m
ρ	=	density of the liquid-vapor mixture, kg/m^3
ρ_d	=	droplet material density, kg/m^3
σ_d	=	droplet surface tension, N/m

Introduction

IN the hot strip rolling mill, temperature control of the strip on the run-out table continues to be the subject of research after years of experimental investigations and experience with different cooling systems.[1–3] The metallurgical properties of the strip and the surface oxide formation depend greatly on the manner in which heat is extracted from the strip. In the conventional hot strip mill where medium to thin strips are produced (2–10 mm in thickness), cooling on the run-out table is normally achieved using laminar water jets. In thin strip casting (1–3 mm in thickness) a new type of cooling system based on mist jets promises to be the most efficient method for cooling. Cooling by mist jets also has several other advantages. It provides uniformity in cooling that leads to improvement in the material properties and the flatness of the rolled product. It is also cost effective because it optimizes the amount of water consumption in the mill.

Spray cooling research has been mainly experimental in nature. A substantial amount of experiments on mist cooling has been performed using single droplet impaction and full sprays. Pederson,[4] Kendall and Rohsenow,[5] Senda et al.,[6] and McGinnis and Holman[7] have studied single-droplet heat transfer. Their findings were very valuable in understanding the cooling effectiveness produced from single impaction. The authors investigated a wide range of surface temperatures that extended from the nucleate boiling to the film boiling range. Other researchers including Sozbir and Yao,[8] Chang and Yao,[9] Ortiz and Gonzalez,[10] Ohkubo and Nishio,[11] and Pais et al.[12] have made heat-transfer measurements using full sprays. They used air-mist nozzles that produced a spectrum of droplet diameters. In all of those experiments, both for single-droplet impaction and air-mist sprays it was found that the heat transfer is dependent on important parameters that include the droplet size, surface temperature, and the droplet Weber number.

Numerically modeling the droplet-wall impaction dynamics and contact heat transfer has not been fully addressed before. Most existing models[13–15] do not consider the droplet bouncing behavior, but only track the droplets up to the point where they make contact with the surface. Also, the droplet partial evaporation at impaction and contact heat transfer was not modeled. A model developed by Nishio and Kim[16] for dilute sprays considers droplets multiple impactions, but the droplet dynamics are assumed to be independent of the droplet velocity and diameter. Furthermore, their model neglects the partial evaporation at the surface and assumes the droplet diameter to remain the same after rebound. In the present report, this is the first time a model is developed to simulate the effect of the impinging droplet Weber number on the droplet-wall dynamics

Received 28 May 2004; revision received 24 November 2004; accepted for publication 14 December 2004.

*Assistant Professor, Department of Mechanical Engineering.
†Professor, Department of Mechanical Engineering.

and on the heat-transfer effectiveness with a realistic comparison to experimental results.

Modeling of Droplet Dynamics

Droplet impingement on the wall can be classified according to the following three main modes of impaction:

Stick mode: This occurs when the droplet approaches the surface with a low impinging Weber number and the droplet adheres to the surface.

Rebound mode: For a higher Weber number, the droplet bounces off the wall after impact. High-speed photography for droplet impingement on a heated surface[17–19] reveals that during impaction the droplet spreads radially in the form of a flattened disk. After the droplet reaches a maximum spread, it begins to recoil backwards towards its center as a result of the surface tension effect. The droplet then rebounds as a long and narrow mass whose shape continuously changes because of the difference in the velocity between the top and bottom parts. The droplet will rebound without breaking up as long as the impinging droplet Weber number is less than the critical Weber number at which the droplet disintegrates. The critical Weber number depends on the surface material properties, especially thermal conductivity, surface roughness, surface temperature, and droplet impingement angle.

Breakup mode: Breakup mode occurs when the droplet impacts the surface at an incoming Weber number equal or greater than the critical Weber number. It has been also found that the number of disintegrated droplets increases with the increase in the Weber number.[20,21]

The surface temperature can have a strong influence on the droplet breakup.[22] For instance, the boiling regime can induce breakup even at a very low impacting energy. In this case, droplets would disintegrate as a result of the rapid liquid boiling on the hot wall accompanied by the formation of gas bubbles blowing through the liquid droplet. If the conditions are favorable for droplets to break up, then depending on the heat-transfer mode various secondary droplet sizes can be formed. Nucleate boiling results in very fine secondary droplet formation, whereas transition boiling results in fine droplet formation, and film boiling results in large size droplet formation.

As mentioned earlier, there are several factors that influence the droplet impaction mode at the wall. However, one factor, which is the Weber number, is considered to be the governing parameter for the droplet deformation. The droplet Weber number is a measure of the relative importance of the droplet kinetic energy (inertial force) to its surface energy (capillary force). Figure 1 explains the nature of impact dynamics for water droplets.[19] At low incoming Weber numbers, the droplets rebound elastically from the wall. As the approach velocity is increased, the normal velocity component of the rebounding droplets decreases sharply because of theradial spread

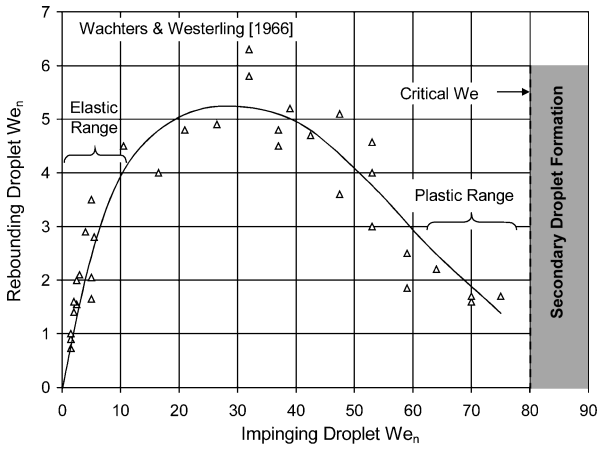

Fig. 1 Relationship between impinging and rebounding We_n (reproduced from Wachters and Westerling[19]).

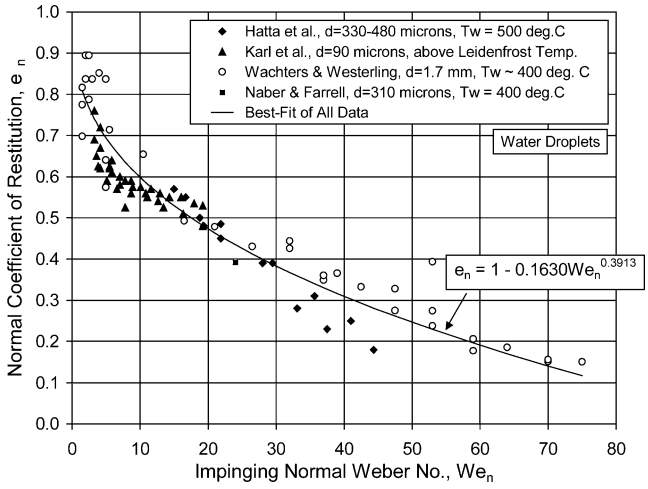

Fig. 2 Water droplet coefficient of restitution as function of We_n at above Leidenfrost temperature (1 atm).

of the droplets over the heated surface. As the rebound velocity becomes very low, the droplet impact mode becomes close to plastic.

The change in the droplet speed and direction during impaction can be quantitatively measured by the normal and tangential coefficient of restitution. Data gathered from Wachters and Westerling,[19] Hatta et al.,[21] Naber and Farrell,[22] and Karl et al.[23] for water droplet impaction at atmospheric conditions (at about Leidenfrost temperature) show the relationship between the droplet normal coefficient of restitution and the droplet normal impinging Weber number (Fig. 2):

$$e_n = 1 - 0.1630We_n^{0.3913} \tag{1}$$

where

$$We_n = \rho_d v_i^2 d/\sigma_d \tag{2}$$

Experiments performed by Karl and Frohn[24] for surfaces heated above the Leidenfrost temperature show the loss in the droplet tangential momentum to the wall to be only about 5%. Recent models for fuel spray-wall impingement in diesel engines have assumed a fixed value of 0.71 for the tangential coefficient of restitution.[25] However, because of the lack of experimental data that relate the tangential coefficient of restitution to the droplet Weber number, the current study assumed the tangential coefficient of restitution to be 1.

Droplets with higher impact energies (i.e., higher Weber numbers) tend to spread more at the surface. According to Chandra and Avedisian,[18] the droplet maximum spread was theoretically shown to be proportional to the square root of the Weber number. Others including Akao et al.,[26] Ueda et al.,[27] and Hatta et al.[20] experimentally showed the droplet spread to be a strong function of the Weber number. For liquid water droplets, the dependency of the droplet spread on Reynolds number is insignificant because of the small viscous losses of water. Experiments conducted by Chandra and Avedisian[18] using n-heptane droplets on a polished stainless-steel surface show that after an early stage of impaction the droplet maximum spread decreases as the wall temperature increases. The contact angle between the droplet and the metal plate is seen to increase from about 24 deg at room surface temperature to about 180 deg at the Leidenfrost temperature, thus resulting in a decrease in droplet spread. Therefore, the momentum loss of the rebounding droplet will also increase with the decrease in surface temperature. As a result, it is expected that the droplet coefficient of restitution for surfaces heated at temperatures ranging from nucleate to film boiling will be lower than that shown in Fig. 2.

Modeling of the Spray Heat Transfer

There are three modes of heat transfer associated with spray cooling (Fig. 3)[14]: 1) boiling heat transfer caused by liquid-solid contact

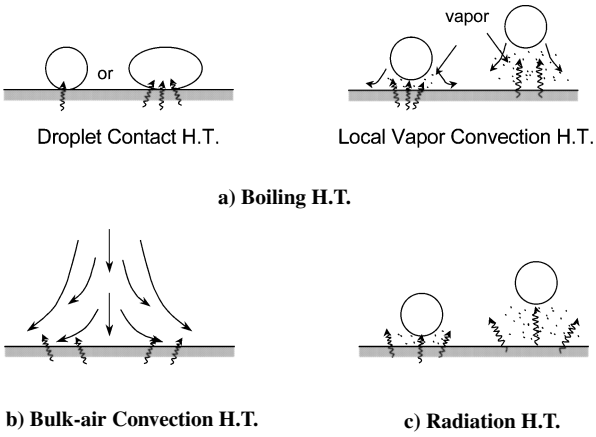

Fig. 3 Spray cooling heat-transfer modes.

(also referred to as contact heat transfer), 2) convection caused by the bulk airflow, and 3) radiation exchange between the heated wall and the two-phase air-water spray mixture. Droplet boiling heat transfer can be classified into two types: 1) heat transfer with wetting contact and 2) heat transfer with nonwetting contact.

For wet cooling, the droplets can be in continuous or semicontinuous direct contact with the wall. After an initial period of transient heat conduction, the droplets enter into either nucleate or transition boiling regimes. In this case, the droplet incoming Weber number can have a weak effect on enhancing the droplet breakup. Wet cooling results in a significant drop in the surface temperature because of its high cooling efficiency.

In nonwet cooling, also referred to as film boiling, the droplet makes contact with the hot surface for a very short period before a vapor film quickly forms between the droplet and the surface.[20] Because vapor has a very low thermal conductivity, it acts as insulation between the surface and the incoming spray, therefore, lowering the cooling efficiency. In this cooling regime, the incoming droplet Weber number has a significant influence on the cooling efficiency. For low Weber numbers, droplets cannot penetrate through the film layer. However, for high-Weber-numbers droplets can penetrate through the film layer, and more surface contact can be established. This enhances the cooling efficiency.

Besides the droplet Weber number and the wall temperature, there are other secondary factors that influence the heat-transfer effectiveness (but not as influential as the Weber number) such as the droplet impingement frequency, surface inclination angle, surface material, and roughness. For surface temperatures below Leidenfrost point, the heat-transfer effectiveness decreases as the droplet impingement frequency increases as a result of the interference between the liquid film layer and the droplets. This effect weakens at temperatures above the Leidenfrost point as a result of the formation of the vapor film layer.[6] An increase in the droplet impingement angle (angle between the droplet motion direction and the normal to the surface) on a horizontal surface lowers the normal component of the Weber number and the heat-transfer effectiveness.[28] This also has a favorable effect on decreasing the interference between the impinging droplets. Highly conductive material increases the heat-transfer rate for surface temperatures below the Leidenfrost point. However, above the Leidenfrost temperature, the high thermal conductivity acts in promoting vapor film generation that leads to isolating the droplets from the surface at a much faster rate.[20] Finally, surface roughness acts favorably in enhancing the heat-transfer rate because the droplet breaks up at a Weber number much lower than the critical Weber number (for disintegration) for a smooth surface.[20]

Pedersen,[4] Senda et al.,[6] and McGinnis and Holman[7] experimentally determined the heat-transfer rate for a single stream of water droplets impinging on a heated metal plate by subtracting the heat-transfer rate with impinging droplets from the heat-transfer rate without the droplets. This net effect excluded the bulk air convective effect, but included the local convective effect caused by the entrainment of the air around the droplet.

The heat transfer associated with the droplet contact with the heated surface can be empirically evaluated using an effectiveness parameter, which is defined as the ratio of the actual heat transfer induced by the droplet to the maximum possible heat transfer that can be achieved:

$$\varepsilon = q_c/G[\Delta h_{\mathrm{fg}} + c_{p,l}(T_{\mathrm{sat}} - T_{\mathrm{liq}}) + c_{p,v}(T_w - T_{\mathrm{sat}})] \qquad (3)$$

The heat-transfer effectiveness is strongly dependent on the impinging Weber number as shown in Figs. 4 and 5 for the wetting and nonwetting boiling regimes, respectively. The heat-transfer effectiveness is at its peak in the nucleate boiling region, but decreases significantly in the film-boiling region. Because the literature data were obtained at the critical maximum (Fig. 4) and minimum (Fig. 5) contact heat fluxes, the heat-transfer effectiveness between these points was interpolated and is presented in Fig. 6 as a function of the Weber number and surface temperature. This figure shows the same behavior depicted by the boiling curve of water and is used to calculate the heat-transfer effectiveness.

Based on the literature review, the following correlation is obtained between the droplet heat-transfer effectiveness and Weber number for the nucleate to film boiling range:

$$\varepsilon = \left(0.10 + 5.2 \times 10^{-4} We_n\right) \cos(\pi/470)[(T_w - T_{\mathrm{liq}}) - 130] + 8.6 \times 10^{-4} We_n + 0.12 \qquad (4)$$

Numerical Scheme

Numerical computations are performed using Fluent (Ver. 5.5), where the control-volume-based approach is used to convert the

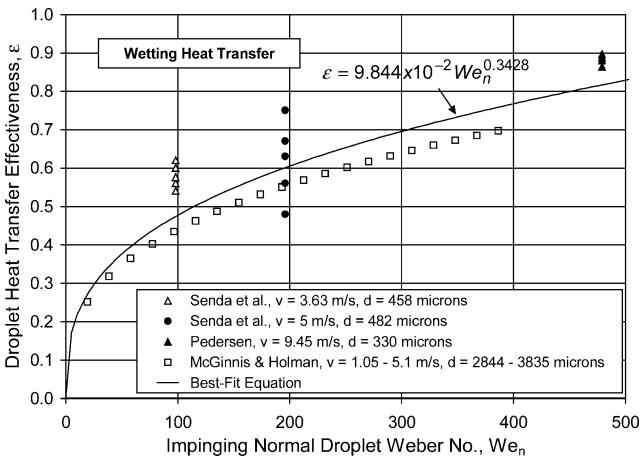

Fig. 4 Water-droplet heat-transfer effectiveness for wet cooling.

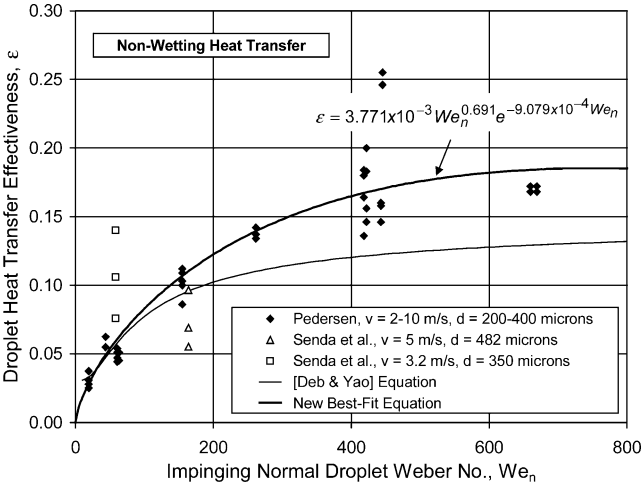

Fig. 5 Water-droplet heat-transfer effectiveness for nonwet cooling.

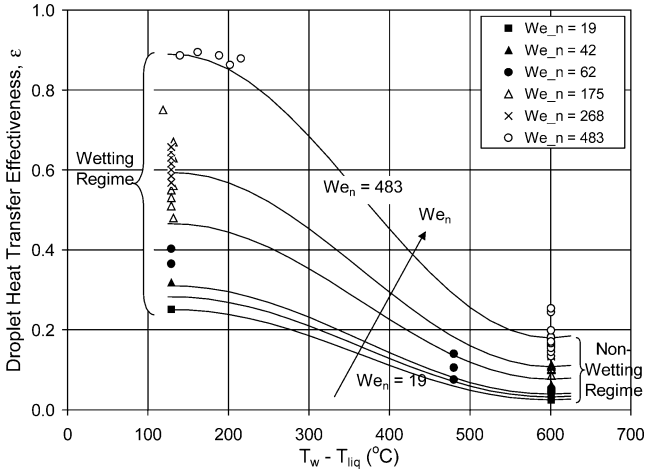

Fig. 6 Water-droplet contact heat-transfer effectiveness in the transition to film boiling region (1 atm).

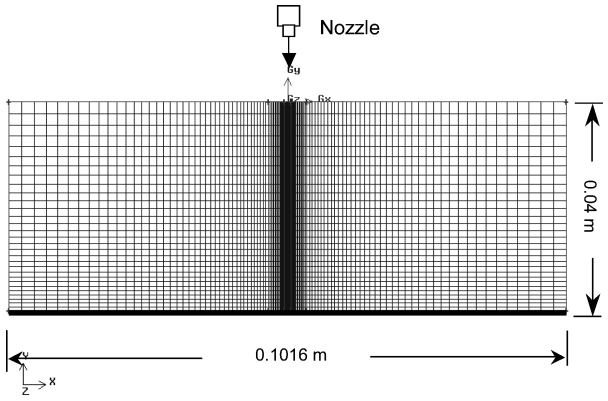

Fig. 7 Grid mesh for the computation domain.

governing equations into algebraic equations that can be then numerically solved. The modeling of the spray consists of a mixture of two phases: an air medium referred to as the continuous phase, and the water droplets referred to as the discrete phase. The droplets are dispersed in the continuous phase and are traced stochastically in the Lagrangian reference frame.

In this model, steady-state flow conditions are simulated. It is assumed that no droplet interaction occurs, and dilute to intermediate dense spray conditions prevail. Also it is assumed that the droplet impinging Weber number is small enough (<80) so that the droplets do not splatter. An axisymmetric model is developed to simulate the spray flow over a heated plate that is 101.6 mm in diameter. The nozzle is situated at the center of the plate at a distance of 40 mm above the plate. Weighting factors are used to concentrate the grid mesh at the center of the computation domain and also near the plate surface (Fig. 7). Sufficient grid refinement at the wall is necessary to capture the wall interaction event and to ensure computational stability. For dilute spray conditions[14] (water mass flux < 2 kg/s · m^2) a quadrilateral grid mesh of 75 × 60 provided acceptable numerical accuracy. However, for higher water mass fluxes a more refined grid mesh was needed. Therefore, the accuracy of the simulation results was grid size dependent, and the grid size that was needed was in turn dependent on the water mass flux. A grid-independence study was conducted, where the density of the nodes near the wall was increased until the solution no longer changed with further grid refinement. To achieve this, an enhanced wall treatment using the two-layer zonal model was enabled in Fluent, where the value of $y^+ (= \rho u_\tau y/\mu)$ at the wall-adjacent cells was kept close to 1. The droplet dynamics and contact heat transfer are modeled using the empirical correlations presented earlier for water droplets. During impaction, the droplet mass is recalculated based on the droplet contact heat-transfer empirical correlations, and the excess mass that is the difference between the incoming droplet mass and the recalculated mass is released as saturated vapor at the nearest cells to the wall. This vapor mass created has the same momentum and energy of the phase from which it is created. The calculations for the droplet dynamic interaction with the wall and the droplet-wall contact heat-transfer effectiveness are introduced into Fluent through user-defined functions, which are complied using a "makefile" that invokes the system C compiler and builds a native object code library. The object code library is linked to Fluent executable software during run time.

The droplet temperature is calculated from an energy balance on the droplet, where the sensible heat change in the droplet is balanced by the convective, radiative, and latent heat transfer between the droplet and the gas-phase medium. Radiation heat transfer is calculated using the P-1 radiation model, which is the simplest case of the more general P-N model.[29] The wall is assumed to be gray and diffuse, where the only radiation boundary condition required is the wall emissivity. The trajectory of the droplet is solved by integrating the force balance on the droplet, where the inertial force is balanced by the drag force and the gravitational force. The drag coefficient between the droplet and air is based on the assumption of a smooth spherical particle and is calculated using the correlation given by Morsi and Alexander.[30] The turbulence continuous-phase model uses the two equations in the k–ε method expressed in Eulerian coordinates. The effect of the gas turbulence on the droplets is obtained by adding a velocity fluctuation to the mean gas velocity while tracing the droplets.

The boundary conditions for the computation domain are as follows. Velocity inlet boundaries are applied for the water droplets and air. The injection plane is considered to be at a small distance below the nozzle-exit plane where the droplets are released. It is assumed that the water stream at this location has been fully atomized. This simplification is necessary to avoid a complicated nozzle model where flow conditions are difficult to simulate. At the vertical edges of the computation domain, pressure outlet boundaries are applied. The wall boundary is assumed to be at a fixed temperature.

The coupling between the droplet-phase and the gas-phase medium is accomplished as follows. The equations for the gas phase are solved prior to the injection of the droplets. The equations for the liquid droplet phase are then introduced, and the trajectories for the droplets are calculated. The effect of the discrete droplets onto the gas-phase is then considered by resolving the gas-phase equations with the newly calculated source terms associated with the presence of the droplets. The droplets trajectories are then recalculated based on the modified results of the gas-phase equations. The procedure is repeated until solution convergence is achieved.

Results and Discussion

Spray Dynamics

The air jet stream and the droplet size have a major influence on the droplet behavior at the wall. For the purpose of visualizing the bouncing behavior of droplets on a heated wall, multiple streams of water droplets ranging from 10 to 200 μm (instead of a full spray) are injected into the middle of the computation domain that is shown in Fig. 7, with the 10 μm at the center and the 200 μm furthest away (see Fig. 8). The results shown in Fig. 8 are based on simulation only. Droplet sizes of 10 to 200 μm are used in this simulation to show the effect of the droplet size on its rebound from the wall. The airflow stream is shown only on the right half of the computation domain. The air and water mass flow rates are 0.028 and 1.2×10^{-3} kg/s. The injection velocity for the air and water droplets is 3 m/s each. The light color lines in Fig. 8 represent the airflow streamlines, while the black lines represent the drop trajectories. The drag force is seen to have a strong influence on the droplet impaction. Larger droplets make it to the surface with a higher impaction velocity, while smaller droplets such as the 10-μm droplet drift away along the heated wall.

The droplet size also influences the frequency of impingements at the wall. Larger droplets retain enough momentum after impact to rebound and impinge again on the surface. The airflow stream also has an effect on the frequency of impingements, and the droplet rebound height. If the air velocity were to be very low, the droplets would impinge on a much smaller area than they would if the air

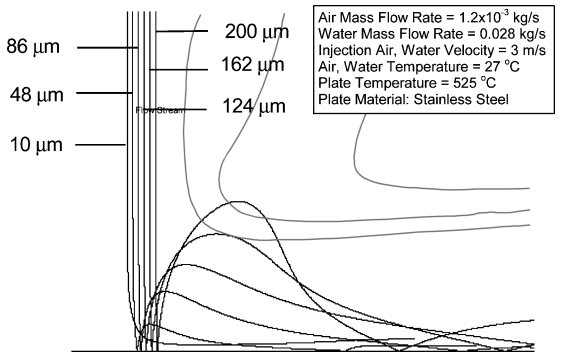

Fig. 8 Surface interaction with various droplet diameters.

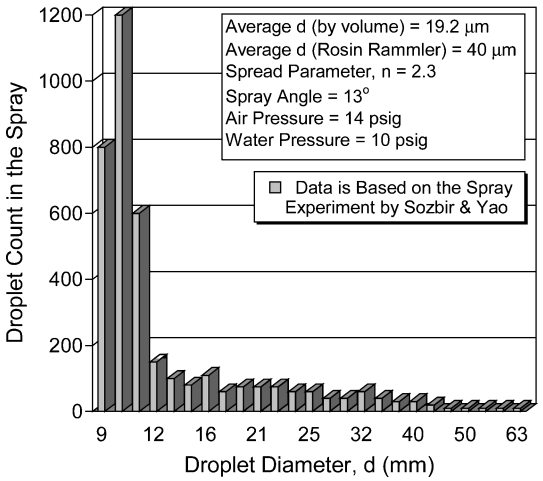

Fig. 9 Droplet count distribution based on the experiment by Sozbir and Yao.[8]

velocity were high. With higher air velocity, the droplets rebound height would be much lower because the airstream tends to push the droplets closer to the wall. It is important to make clear that the droplet bouncing behavior on the heated wall is based on a correlation for test data at near the Leidenfrost temperature. For wall temperatures in the nucleate or transition boiling range, the droplet is expected to have a lower coefficient of restitution than that shown in Fig. 2 because of the increase in the droplet spread at the wall and also the increase in the evaporation rate at contact. Therefore, simulation of the droplet/wall dynamic behavior conducted at the nucleate or transition-boiling temperatures using the correlation in Fig. 2 should be considered with some reservation.

Heat-Transfer Phenomena

The current spray model was developed based on the fundamental basics of single-droplet impingements extended to full sprays. To check its validity, the model is tested by simulating the spray experiment that was conducted by Chang and Yao.[9] A full conical spray type is injected on a stainless-steel plate of 101.6 mm in diameter heated to 525°C. The nozzle system consists of an air-mist nozzle (by Spraying Systems) surrounded by an air chamber. The reason for the extra airflow is to produce finer droplet size in the spray. The initial air and droplet temperature is 27°C. The air and water mass flow rates are 2×10^{-3} and 10^{-4} kg/s (20:1 ratio), respectively. The nozzle system is situated at 40 mm above the plate and oriented such that the air-mist flow hits the plate perpendicularly at the stagnation point. The air velocity exiting the air chamber is 35 m/s. The air-mist nozzle has an exit diameter of 7.9 mm. The liquid flow flux at the plate center (stagnation point) is 2.5 kg/m^{2}s at 1-atmo ambient pressure. For these flow parameters, the nozzle spray angle was 13 deg. The spray has a spectrum of droplet diameters with an average diameter of 19.2 μm by volume, a minimum of 9 μm, and a maximum of 63 μm as shown in Fig. 9 (Ref. 8).

Figure 10 shows the simulation of the spray mist in Fluent. On the order of a few thousand particle streams were injected to simulate the actual spray. The size of the injected droplets was based on a Rosin–Rammler distribution of the actual test data. Simulation shows that the impinging droplet Weber number (for the spray) on impaction with the surface ranged between nine for the smallest droplet to slightly above 80 for the largest diameter. Figure 11 shows a comparison between the simulated test and Chang's experimental data. The model was first tested to simulate the profile of the bulk air heat-transfer coefficient along the plate radius. As shown in Fig. 11, the model results compared very well with the experimental data. Next, water droplets were injected with the airstream, and the results were also promising. The only deviation in the data occurred towards the edge of the plate where the model predicted fewer droplets to surface interaction. Using the multisize droplet spectrum (Fig. 9), the droplets contact the wall at random locations with the largest hitting in the vicinity of the jet impingement point and the smaller droplets hitting further away, resulting in very uniform cooling. The numerical heat-transfer coefficient shown in Fig. 11 is obtained from Fluent results. In the current simulation, radiation heat transfer contributed to about 5% of the total heat transfer.

Figure 12 shows a comparison between the mist heat-transfer coefficient as calculated using the model vs the test data by Chang and Yao[9] for different liquid mass fluxes. The studies conducted by Chang and Yao show that for a light liquid loading the heat transfer of the mist-wall contacts and that of the bulk air convection can be proven to be independent. In the current simulation, the mist

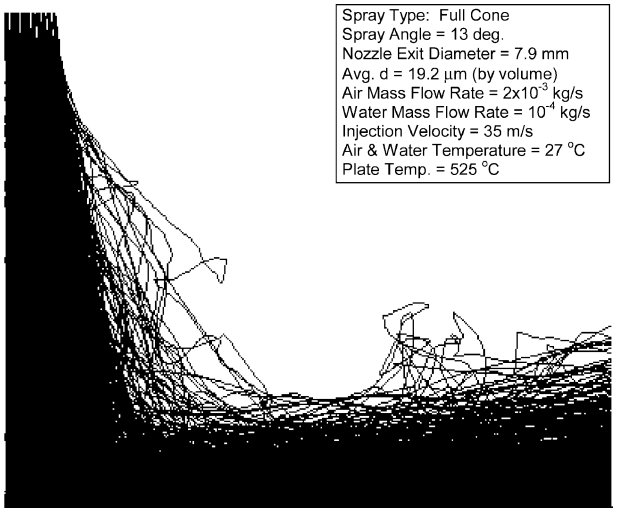

Fig. 10 Mist spray pattern at 1-atm ambient pressure (Avg. $d = 19.2$ μm by volume).

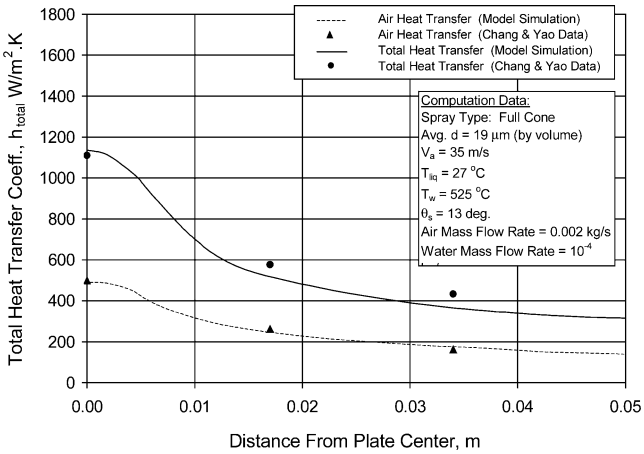

Fig. 11 Simulation of the total heat-transfer coefficient vs actual test data for a conical spray.

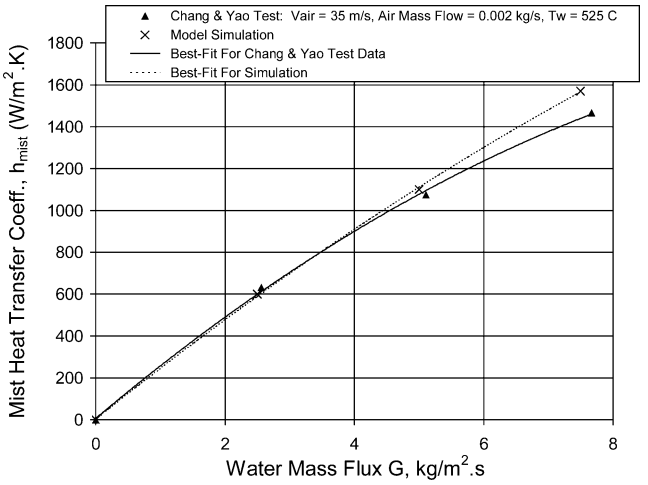

Fig. 12 Mist heat transfer vs water mass flux.

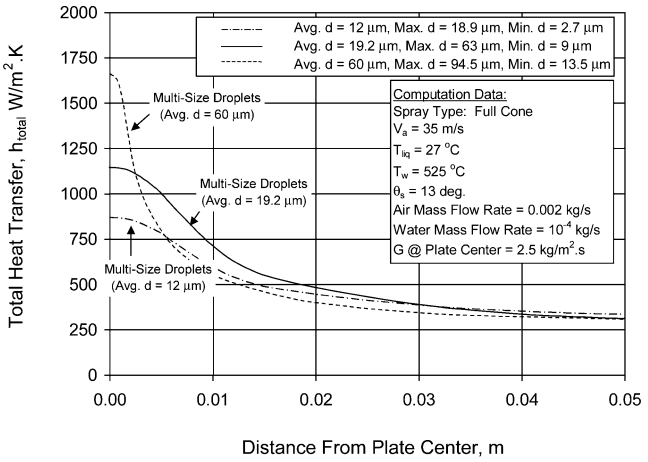

Fig. 13 Cooling profile using various multisize droplets spray.

heat transfer included the droplet boiling heat transfer and the local convective effects caused by the presence of the droplets, while the bulk air heat transfer was due only to the forced airflow without the droplets. For low mass fluxes, the almost linear relationship between the mist heat-transfer coefficient and the liquid mass flux shows the spray behaves like an ideal one, and the likelihood of droplets interaction is very small. The deviation between the calculated and test data occurred at higher liquid mass fluxes (>4 kg/m^2 · s) because of the flooding (which is detrimental to the heat transfer) that becomes significant at higher mass fluxes. The current numerical model does not correct for the flooding and therefore overpredicts the cooling heat transfer for dense sprays.

Figure 13 shows the effect of the spray average droplet size on the cooling profile using a spray that has a spectrum of droplet sizes. The three cases shown in Fig. 13 for the multisize droplet spectrums have the same Rosin–Rammler spread. For a spray whose average droplet size is large (such as the case of a multisize droplet distribution with an average droplet size of 60 μm), for the same liquid mass flux the droplet density will be low, and the droplets will contact the wall at scarce locations with the largest droplets in the vicinity of the jet impingement point (stagnation point) because of the high droplet inertia. Thus, the heat-transfer profile will be nonuniform with extreme cooling around the jet impingement point. On the other hand, for the same liquid mass flux but with a smaller average droplet size (such as the case of a multisize droplet distribution with an average droplet size of 19 μm) the droplet number density will be much higher and so would be the droplet surface to wall surface contact area. Therefore, the cooling will be more uniform.

Conclusions

A numerical model based on the Lagrangian tracking of droplets was developed for the purpose of studying the mist cooling on metallic surfaces. Numerically modeling the droplet-wall impaction dynamics and contact heat transfer has not been addressed before. This is the first time a model is developed to simulate the effect of droplet Weber number on the droplet-wall multiple impaction and on the droplet contact heat-transfer effectiveness. The current model is based on the fundamental basics of single droplet impaction extended to full sprays. The model assumes that no droplet interaction occurs and that the droplets do not break apart after impaction. The model was tested using experimental data for nozzles that dispense a wide spectrum of nonuniform droplets. Parametric studies conducted using the current model reveal the following important issues:

1) The air velocity and droplet diameter strongly affect the dynamic behavior of the droplet at the wall. Because of the higher momentum, larger droplets impinge closer to the stagnation point, whereas smaller droplets impinge further away. Larger droplets retain enough of their initial momentum to reimpinge back again. It was also revealed that sprays with large average droplet sizes could have a ballistic and localized impaction near the stagnation point.

2) The cooling profile depends on the droplet size distribution of the air-mist spray. Sprays dispersing a wide spectrum of droplet sizes and whose average size is large result in a nonuniform cooling profile with a high cooling in the center of the plate and very little cooling around the edges. On the other hand, sprays whose average droplet size is small result in a uniform cooling profile. This is because for the same mass flux the droplet number density will be much higher and so would be the surface-to-surface contact area between the droplets and the wall. However if the droplets are too small, they will cool the air but might not make contact with the surface. As a result, the cooling will be very uniform but stretch over a very long path.

References

[1]Evans, J. F., Roebuck, I. D., and Watkins, H. R., "Numerical Modeling of Hot Strip Mill Runout Table Cooling," *Iron and Steel Engineer*, Vol. 70, No. 1, Jan. 1993, pp. 50–55.

[2]Ishida, R., Mizuta, A., Korida, K., Yasunaga, S., and Takisawa, K., "Basic Characteristics of Pipe Nozzle Cooling with Retaining Water on Plate," *ISIJ International*, Vol. 29, No. 4, 1989, pp. 339–344.

[3]Hadrian, U. T., "The Cooling Efficiency of Laminar-Orthogonal Water (LOW) Curtains in Hot Strip Mills," *Metallurgical Plant and Technology*, Vol. 7, No. 6, 1984, pp. 44–49.

[4]Pedersen, C. O., "An Experimental Study of the Dynamic Behavior and Heat Transfer Characteristics of Water Droplets Impinging Upon a Heated Surface," *International Journal of Heat and Mass Transfer*, Vol. 13, No. 2, 1970, pp. 369–381.

[5]Kendall, G. E., and Rohsenow, W. M., "Heat Transfer to Impacting Drops and Post Critical Heat Flux Dispersed Flow," Heat Transfer Lab., Massachusetts Inst. of Technology, Technical Report 85694-100, Cambridge, March 1978.

[6]Senda, J., Yamada, K., Fujimoto, H., and Miki, H., "The Heat Transfer Characteristics of a Small Droplet Impinging upon a Hot Surface," *JSME International Journal, Series II*, Vol. 31, No. 1, 1988, pp. 105–111.

[7]McGinnis, F. K., III, and Holman, J. P., "Individual Droplet Heat Transfer Rates for Splattering on Hot Surfaces," *International Journal of Heat and Mass Transfer*, Vol. 12, No. 1, 1969, pp. 95–108.

[8]Sozbir, N., and Yao, S. C., "Experimental Investigation of Water Mist Cooling for Glass Tempering," *Atomization and Sprays*, Vol. 14, No. 3, 2004, pp. 191–210.

[9]Chang, Y. W., and Yao, S. C., "Studies of Water Mist Cooling on Heated Metal Surfaces," *Proceedings of NHTC'00, 34th National Heat Transfer Conference*, Vol. 1, edited by S. C. Yao and A. Jones, American Society of Mechanical Engineers, New York, 2000, pp. 683–690.

[10]Ortiz, L., and Gonzalez, J. E., "Experiments on Steady-State High Heat Fluxes Using Spray Cooling," *Experimental Heat Transfer*, Vol. 12, No. 3, 1999, pp. 215–233.

[11]Ohkubo, H., and Nishio, S., "Study on Transient Characteristics of Mist-Cooling Heat Transfer from a Horizontal Upward-Facing Surface," *Heat Transfer—Japanese Research*, Vol. 21, No. 6, 1992, pp. 543–555.

[12]Pais, M. R., Chow, L. C., and Mahefkey, E. T., "Surface Roughness and Its Effects on the Heat Transfer Mechanism in Spray Cooling," *Journal of Heat Transfer*, Vol. 114, No. 1, 1992, pp. 211–219.

[13]Liu, L., and Yao, S. C., "Heat Transfer Analysis of Droplet Flow Impinging on a Hot Surface," *Proceedings of the Seventh International Heat Transfer Conference*, Vol. 4, edited by U. Grigvll, Hemisphere, New York, 1982, pp. 161–166.

[14]Deb, S., and Yao, S. C., "Analysis on Film Boiling Heat Transfer of Impacting Sprays," *International Journal of Heat and Mass Transfer*, Vol. 32, No. 11, 1989, pp. 2099–2112.

[15]Delcorio, B., and Choi, K. J., "Analysis of Direct Liquid-Solid Contact Heat Transfer in Monodispersed Spray Cooling," *Journal of Thermophysics Heat Transfer*, Vol. 5, No. 4, 1991, pp. 613–620.

[16]Nishio, S., and Kim, Y. C., "Heat Transfer of Dilute Spray Impinging on a Hot Surface," *International Journal of Heat and Mass Transfer*, Vol. 41, No. 24, 1998, pp. 4113–4119.

[17]Makino, K., and Michiyoshi, I., "The Behavior of a Water Droplet on Heated Surfaces," *International Journal of Heat and Mass Transfer*, Vol. 27, No. 5, 1984, pp. 781–791.

[18]Chandra, S., and Avedisian, C. T., "On the Collision of a Droplet with a Solid Surface," *Proceedings of the Royal Society of London A*, Vol. 432, No. 1884, 1991, pp. 13–41.

[19]Wachters, L. H. J., and Westerling, N. A. J., "The Heat Transfer from a Hot Wall to Impinging Water Drops in the Spheroidal State," *Chemical Engineering Science*, Vol. 21, No. 11, 1966, pp. 1047–1056.

[20]Hatta, N., Fujimoto, H., Kinoshita, K., and Takuda, H., "Experimental Study of Deformation Mechanism of a Water Droplet Impinging on Hot Metallic Surfaces Above the Leidenfrost Temperature," *Journal of Fluids Engineering*, Vol. 119, No. 3, 1997, pp. 692–699.

[21]Hatta, N., Fujimoto, H., Takuda, H., Kinoshita, K., and Takahashi, O., "Collision Dynamics of a Water Droplet Impinging on a Rigid Surface above the Leidenfrost Temperature," *ISIJ International*, Vol. 35, No. 1, 1995, pp. 50–55.

[22]Naber, J. D., and Farrell, P. V., "Hydrodynamics of Droplet Impingement on a Heated Surface," Society of Automotive Engineers, Publication 930919, March 1993.

[23]Karl, A., Rieber, M., Schelkle, M., Anders, K., and Frohn, A., "Comparison of New Numerical Results for Droplet Wall Interactions with Experimental Results," *ASME 1996 Fluids Engineering Division Conference*, Vol. 1, edited by H. W. Coleman and C. T. Crowe, American Society of Mechanical Engineers, New York, 1996, pp. 201–206.

[24]Karl, A., and Frohn, A., "Experimental Investigation of Interaction Processes Between Droplets and Hot Walls," *Physics of Fluids*, American Inst. of Physics, Melville, NY, Vol. 12, No. 4, 2000, pp. 785–796.

[25]Lee, S. H., and Ryou, H. S., "Development of a New Spray/Wall Interaction Model," *International Journal of Multiphase Flow*, Vol. 26, No. 7, 2000, pp. 1209–1234.

[26]Akao, F., Araki, K., Mori, S., and Moriyama, A., "Deformation Behaviors of a Liquid Droplet Impinging onto Hot Metal Surface," *Transactions of Iron and Steel Institute of Japan*, Vol. 20, No. 11, 1980, pp. 737–743.

[27]Ueda, T., Enomoto, T., and Kanetsuki, M., "Heat Transfer Characteristics and Dynamic Behavior of Saturated Droplets Impinging on a Heated Vertical Surface," *Bulletin of the JSME*, Vol. 22, No. 167, 1979, pp. 724–732.

[28]Shi, M. H., Bai, T. C., and Yu, J., "Dynamic Behavior and Heat Transfer of a Liquid Droplet Impinging on a Solid Surface," *Experimental Thermal and Fluid Science*, Vol. 6, No. 2, 1993, pp. 202–207.

[29]Siegel, R., and Howell, J. R., *Thermal Radiation Heat Transfer*, Hemisphere, Washington, D.C., 1992, Chap. 16.

[30]Morsi, S. A., and Alexander, A. J., "An Investigation of Particle Trajectories in Two-Phase Flow Systems," *Journal of Fluid Mechanics*, Vol. 55, No. 2, 1972, pp. 193–208.